# Design and Development of PSO-Firefly Hybrid Optimizer–CNN Model for Lung Disease Classification using Chest X-Ray Images

Tanu Dhiman[1,*], Puneet Kumar[1]

[1]Department of Computer Science & Engineering, Chandigarh University, Mohali, Punjab 140301, India

*Author to whom correspondence should be addressed:
E-mail: tanudhiman0707@gmail.com

(Received May 02, 2025; Revised October 14, 2025; Accepted March 16, 2026)

**Abstract**: Lung diseases such as Pneumonia, COVID-19, and Tuberculosis (TB) are major contributors to global mortality, making early and accurate diagnosis crucial for effective treatment. This paper introduces a novel Hybrid Nature-Inspired Optimizer – Convolutional Neural Network (HNI-CNN) model for the classification of lung diseases from chest X-ray images. The model integrates Particle Swarm Optimization (PSO) and Firefly Algorithm (FFA) to form a hybrid feature selection method, which optimizes the extraction of relevant features, significantly enhancing the classification accuracy. Additionally, Principal Component Analysis (PCA) is employed to reduce dimensionality, ensuring the model focuses on the most informative features. Tested on the Kaggle lung disease dataset, the HNI-CNN model achieves state-of-the-art performance, with an accuracy of 98.0%, precision of 96.8%, and recall of 99.0%, outperforming leading models such as NasNetMobile, MobileNetV2, and EfficientNetB1. This research presents a significant advancement in intelligent diagnostic systems by offering a more reliable and efficient method for feature selection and classification. The hybrid optimization approach not only improves performance but also enhances the robustness of automated medical diagnostics, making it a valuable tool for expert systems in healthcare.

**Keywords:** Deep Learning; Hybrid Optimizer with nature-inspired component –convolutional neural network (HNI-CNN); Lung X-ray Images; Medical Imaging

## 1. Introduction

Lungs are crucial for the human system, facilitating oxygen and carbon dioxide exchange. Lung diseases affect breathing organs and tissues, leading to airway, lung tissue, and circulation issues. Common colds and influenza cause mild discomfort, while pneumonia, tuberculosis, and lung cancer cause severe acute respiratory problems. Radiology diagnoses lung disease by determining patterns, locations, and geographical distribution, using the lungs' ability to embrace, and interchange O2 and CO2 as a diagnostic tool[1)]. Lung disease, a global health concern, causes 7.1 million people to pass away annually, which places it fourth globally. Improved outcomes can be achieved by identifying lung diseases early and managing them effectively. These diseases include a variety of infections that injury the lungs and their function. Lung diseases are triggered by factors like smoking, air pollution, genetic diseases, infections, and auto immune diseases. Patient mortality can be decreased and outcomes can be enhanced with early diagnosis and handling of lung disorders brought on by viruses, unhealthy dietary habits, and genetics. Reactive airway disease, a condition causing inflammation and narrowing of the lungs' airways, can cause difficulty breathing before the diagnosis of obstructive pulmonary disease[2)]. The lungs, located at the diaphragm and below Figure 1, the rib cage, are crucial for waste disposal and the respiratory system. They can be affected by conditions, drugs, infections, and workplace exposure, with radiology aiding diagnosis. Common lung diseases like asthma, pneumonia, COVID-19, etc., cause signs and symptoms like coughing, minimum breath, chest pain, and tiredness, requiring medical attention. Pneumonia inflames air sacs and can be severe, especially for the elderly and children.

Environmental, climate change, and lifestyle factors are contributing to an increase in premature lung diseases, particularly in developing and low-middle-income countries, resulting in over 4 million deaths annually. To combat this, it is vital to diminish air pollution and carbon emissions, implement efficient diagnostic systems, and

Cite: T. Dhiman, P. Kumar, "Design and Development of PSO-Firefly Hybrid Optimizer-CNN Model for Lung Disease Classification using Chest X-Ray Images". Evergreen, 13 (01) 280-293 (2026). https://doi.org/10.5109/7411069.

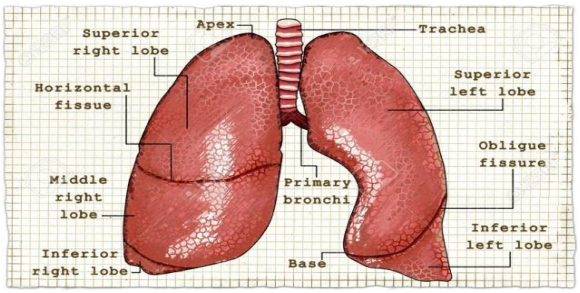


**Fig. 1:** Lung Anatomy

implement early detection methods. The COVID-19 pandemic has exacerbated lung damage and breathing problems, Tuberculosis, caused by Mycobacterium tuberculosis, can affect the lungs, spine, brain, and kidneys[3]. When someone coughs, sneezes, or talks, respiratory droplets are the main way that COVID-19, a virus similar to SARS-CoV-2, spreads. Based mostly on the coronavirus family virus, COVID-19, which started in Wuhan, China, claimed about 5.2 million lives worldwide by December 2021. The virus, also known as SARS-CoV-2, is highly contagious and transmits through exhaling droplets. Its global impact is exacerbated by government restrictions aimed at preventing exposure to the virus[4]. COVID-19 causes pneumonia, causing lung inflammation and respiratory difficulties, particularly for weakened immune systems and those with underlying health conditions. Seek medical attention if symptoms persist[5]. The COVID-19 diagnosis is typically linked to pneumonia symptoms and chest or lung X-ray tests, which are the initial phase imaging methods to play a significant role in the disease's analysis. A negative chest or lung X-ray can indicate COVID-19 or SARS[6].

## 1.1. Contribution and Organization of paper

The contributions of this study are recapitulated as follows:

- Proposed an hybrid HNI-CNN model to classify or detect the disease categories efficiently and precisely.
- The research approach utilizes a PCA for feature extraction, hybridization using PSO and Firefly Optimization, and a CNN classifier used for the detection the lung chest X-ray Images. PSO is known for its simplicity and efficiency in exploring large search spaces, while FFA is good for local optimization and fine-tuning solutions. PSO's global search capability can help explore a broader feature space, while FFA can refine and exploit promising regions identified by PSO.
- Review and compare the performance of the proposed hybrid HNI-CNN model with the state of the art methods.
- Integration of PSO and FFA for feature selection in the context of lung disease classification is a novel approach and is not commonly applied together in existing literature, which sets our work apart.

The remaining sections of the paper is organized as follows. The current and previous reviews are defined in Section 2, and the steps of the research technique are covered in Section 3. The research work is defined in Section 4. The examination of the simulation results and the comparative analysis are covered in Section 5. Section 6 offered the summary and scope for the future.

## 1.2. Background and Related work

Several existing researchers are exploring machine learning and DL schemes for predicting X-ray image diagnostic information, as computers and vast records are unrestricted, making it crucial to address this issue. Mahmud and his colleagues implemented the DL technique for COVID-19 and pneumonia infection classification using CovXNet, achieving 96.9% accuracy in a public dataset[7]. Ibrahim and his colleagues established a binary classification approach for COVID-19. For this motive, around 7232 CXR images were utilized and four DL models using various evaluation parameters[8]. Li and his colleagues presented the COVID-19 detection technique which achieved better results in differentiating between pneumonia produced by COVID-19 and pneumonia obtained from the community[9]. Panwar and his colleague developed COVnet, a 24-layer CNN model that accurately classifies COVID-19 and normal images using a CXR image dataset achieving up to 97% accuracy[10].

The main objectives of this proposed work are defined as below:

- In this research work, the implemented approach is the design of different lung chest X-ray images with a hybrid optimizer with nature-inspired components using the CNN model technique.
- The method involves different phases such as pre-processing, data augmentation, feature extraction, hybrid feature selection, and detection.
- The novel work of the preprocessing phase involves improving the actual uploaded images of lung X-ray images for extracting the data by identifying the undesired noises. Then, it evaluates the smooth image using a median filter.
- After, the pre-processing phase the feature extraction approach extracts the reliable features from the improved images using the principal component analysis (PCA) algorithm. This feature extraction technique is used to extract reliable feature vectors.
- After that feature extraction, it introduced and proposed a hybrid feature selection method using particle swarm optimization (PSO) and Firefly optimization (FFA) algorithms. It has selected the valuable feature sets with the help of objective function. Then, it implemented a convolutional neural network method to detect and classify the

Cite: T. Dhiman, P. Kumar, "Design and Development of PSO-Firefly Hybrid Optimizer-CNN Model for Lung Disease Classification using Chest X-Ray Images". Evergreen, 13 (01) 280-293 (2026). https://doi.org/10.5109/7411069.

disease.

- This research work has introduced a hybrid optimizer with a nature-inspired component CNN model (HNI-CNN). After the evaluation distinct metrics like accuracy, precision, recall, and mean square error rate.

## 1.3. Related Work

Recent advances in deep learning (DL) have substantially improved the automated diagnosis of pulmonary diseasl.'es from chest X-ray (CXR) images. Early works by Bharati et al. demonstrated the potential of deep convolutional architectures such as VGG, ResNet, and DenseNet for identifying complex lung pathologies. Their hybrid VGG–STN–CNN framework effectively extracted high-level features and achieved superior performance on the NIH dataset, with the VDSNet model attaining 73% validation accuracy[4)].

Similarly, Khan et al. utilized three fine-tuned pre-trained networks to detect COVID-19 infections, showing that DL-based radiographic screening could complement PCR testing as a safer and faster diagnostic alternative[5)].

Among these, EfficientNet-B1 achieved 96.13% accuracy in classifying disease and non-disease cases[11)].

Several researchers explored transfer learning and model optimization for robust feature extraction. Abbas et al. proposed the DeTrac framework using pre-trained CNNs and fine-tuning strategies to classify COVID-19 with 93.1% accuracy[12)].

Ali et al. compared six architectures—InceptionResNetV2, Xception, VGG16, ResNet50, and EfficientNetV2L—achieving accuracies between 87.78% and 94.02% for pneumonia detection[13)].

Bakir et al. developed an artificial neural network (ANN) for multi-class lung disease classification, outperforming CNN and SVM baselines with 95.67% accuracy in binary tasks[14)].

Makris et al. demonstrated that transfer learning-based models can rapidly detect COVID-19 cases with up to 95% accuracy, underscoring the utility of AI-driven screening in pandemic scenarios[15,16)].

Recent studies further enhanced classification reliability through feature fusion and ensemble learning. Ji et al. employed multi-modal feature fusion with small-sample enhancement, using global average pooling and fine-tuning to outperform traditional models in COVID-19 detection[17,18)].

Constantinou et al. validated five deep CNNs on a large public dataset, where ResNet101 achieved 96% accuracy[19)]. Kundu et al. applied deep transfer learning with a weighted ensemble of three CNNs, obtaining high accuracy and sensitivity on Kermany and RSNA datasets[20)].

Similarly, Ismael and Şengür showed that CNNs such as VGG16, ResNet50, and InceptionV3 provided rapid COVID-19 screening from X-rays, addressing testing delays during the pandemic[21)].

Hybrid and optimized CNN architectures continue to show strong potential. Gupta et al. designed a hybrid CNN to detect COVID-19 and pneumonia, achieving 97.3% accuracy[22)].

Alqudah et al. combined deep CNNs (AOCTNet, MobileNet, ShuffleNet) with traditional classifiers such as SVM and Random Forest for robust COVID-19 diagnosis[23)].

Houby utilizes pre-trained convolutional neural network models under a transfer learning framework to analyze chest X-ray images for COVID-19 classificationThe approach demonstrates strong performance, achieving around 95% accuracy along with high precision and recall[24)].

Heidari et. al. proposed the approach which achieves improved classification performance, reporting accuracy of approximately 96% with better sensitivity and specificity[25)].

Ibrahim et al. used AlexNet for three-way pneumonia classification, attaining 94.43% accuracy and suggesting that combining CNN with SVM or SVR further improves performance[8)].

Using Xception architecture, Khan et al. identified viral and bacterial pneumonia with high accuracy, while other CNN-based models achieved competitive sensitivity and specificity with minimal computational cost[26–28)]. Ucar and Korkmaz further optimized the SqueezeNet architecture

**Table 1:** Analysis of various existing methods based on lung-related diseases

| Reference | Method / Model | Dataset Used | Reported Accuracy | Key Limitation |
|---|---|---|---|---|
| Mahmud et al. (2020) | CovXNet | Public COVID-19 Dataset | 96.90% | Small dataset, limited generalization |
| Ibrahim et al. (2024) | Binary DL Classifier | 7232 CXRs | 94.40% | Limited class diversity |
| Panwar et al. (2020) | COVnet (24-layer CNN) | COVID-19 vs Normal | 97% | No feature optimization |
| Khan et al. (2022) | Pretrained DL Models | COVID-19 Dataset | ~95% | No hybrid optimization |
| Gupta et al. (2023) | Hybrid CNN | COVID-19 + Pneumonia | 97.30% | Limited dataset diversity |
| Proposed Work (HNI-CNN) | PCA + PSO+FFA + CNN | Combined Public Datasets | 98.00% | Requires broader validation |

Cite: T. Dhiman, P. Kumar, "Design and Development of PSO-Firefly Hybrid Optimizer-CNN Model for Lung Disease Classification using Chest X-Ray Images". Evergreen, 13 (01) 280-293 (2026). https://doi.org/10.5109/7411069.

with Bayesian optimization to enhance COVID-19 classification performance[29,30].

Overall, these studies demonstrate that deep learning and hybrid optimization frameworks substantially improve the accuracy, robustness, and interpretability of lung disease classification using CXR images, analysis of the same is shown in Table 1. However, most existing works rely on single optimizers or standard CNNs, motivating the need for hybrid, nature-inspired optimization–driven models (like PSO–FFA–CNN) that can better balance feature selection, convergence, and diagnostic reliability.

### 1.4. Challenges and Issues

This section highlights major four main issues in DL for lung disease detection: data imbalance, manage large image sizes, limited databases, and maximum error correlation. These challenges are crucial for developing accurate models. Future research should focus on improving data balance, optimizing image processing, expanding datasets, and mitigating error correlation.

#### 1.4.1. Data Imbalance

Data imbalance in classification training can lead to biased models, as the count of images in single class is often advanced than the other. This imbalance can result in the model favoring the majority class and producing inaccurate predictions for the minority class. Techniques like oversampling or under-sampling can address this issue, but it's often not the case. Balancing the dataset for COVID-19, pneumonia, and normal lungs is crucial for accurate and reliable models, as pneumonia often has more images than COVID-19.

#### 1.4.2. Handling Huge Image Size

To lower computational costs and improve processing speed and efficiency; researchers have shrunk the real image size through training. This can be achieved through cropping or resizing images to fit memory constraints, as training with the real image size is expensive and time-consuming, even with potent GPU hardware. This approach also prevents overfitting and enhances model generalization performance.

#### 1.4.3. Limited Available Datasets

Researchers often struggle with limited datasets, leading to the search for alternative methods to produce a good classifier. In transfer learning (TL), a pre-trained method is refined on a smaller database for improved performance, whereas in data augmentation, pre-existing images are altered to generate additional training examples.

#### 1.4.4. High Correlation of Errors

Ensemble methods often face a high correlation of errors due to similar base classifiers making similar mistakes. To improve performance, diversity in base classifiers can be introduced, with low correlation ensuring varied errors. Training them on different data or algorithms can increase diversity and reduce error correlation. Future research should explore ensembles with diverse features or different algorithms to enhance accuracy.

## 2. Proposed Methodology

The flow of the proposed architecture shows various modules and sub-modules to process and analyse the medical image samples. It helps the proposed architecture classify the infection in medical images.

The proposed architecture in Figure 2 shows the various modules like uploading, pre-processing of the medical images, Feature extraction with optimized feature-based technique, and training and testing of models. The pre-processing module provides the best quality of the uploaded sample for visible infection in medical images. The pre-processed sample extracted the disease view features based on the PCA method and processed them with training and testing modules. Table 2 shows the hypermeters & setting used for implementing the proposed work.

The training module uses the sample labeled values of the features given in the training dataset. It helps to find the infected and non-infected examples in the dataset and makes the system understand the features of the infected samples well. The labeled samples are used to train the enhanced proposed model and load on the testing side to classify the test phase processed samples. The decision layer in the proposed architecture Hybrid optimizer with Nature-inspired component CNN model (HNI-CNN) shows classified results of infected and non-infected samples and helps find the disease in patients from the testing phase. The detailed description of all phases are defined in the subsequent subdivisions[31].

**Table 2:** Hyperparameters & Training Settings

| Parameter | Value |
|---|---|
| Learning rate | 0.001 |
| Optimizer | Adam |
| Batch size | 32 |
| Epochs | 100 |
| Early stopping | Yes |

### 2.1. Dataset & Split

A dataset of lung-based chest X-ray (CXR) pictures for COVID-19 positive cases, coupled with normal and viral pneumonia images, has been created by Doha and Bangladeshi medical professionals[32].

This COVID-19, other lung infection, and normal dataset is unconfined in phases. Initial update they have improved the COVID-19 class to 1200 lung x-ray images. The dataset has been enhanced to include 3616 COVID-19 positive patients, 10,192 normal, 6012 lung opacity (a lung illness unrelated to COVID-19), and 1345 viral pneumonia

photos in the another update[33]). As shown in Table 3, the dataset consists of four classes with balanced distribution across training, validation, and testing sets, ensuring reliable model evaluation.

A 70:15:15 (70% for training, 15% for validation, and 15% for testing) patient-level split was applied, ensuring no overlap between sets. Figure 3. illustrates the data flow from raw dataset → preprocessing → final splits.

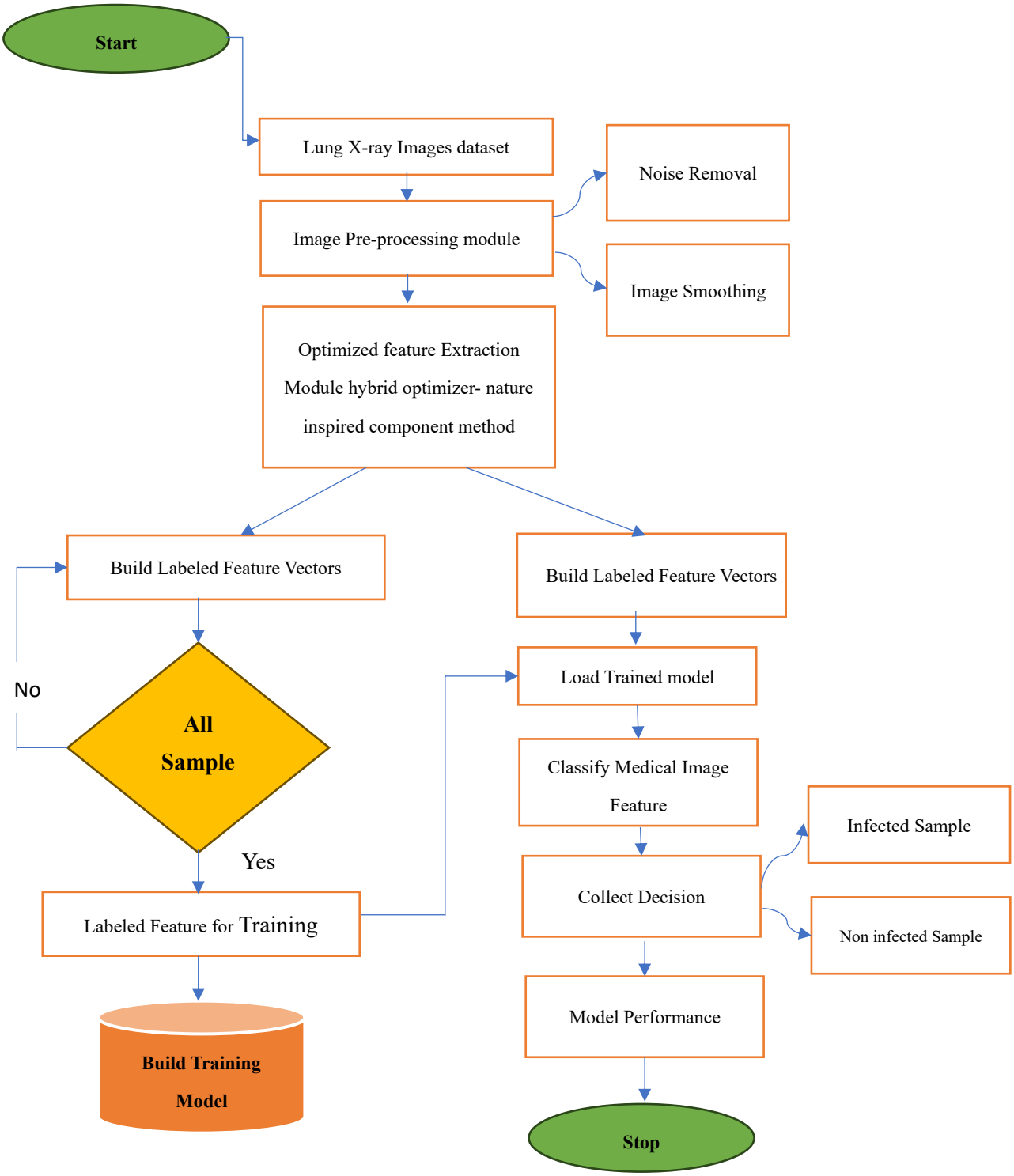


**Fig. 2:** Proposed Workflow

**Table 3:** Dataset Summary

| Class | Training | Validation | Testing | Total |
|---|---|---|---|---|
| COVID-19 | 2531 | 542 | 543 | 3616 |
| Normal | 7134 | 1529 | 1529 | 10,192 |
| Pneumonia | 4210 | 901 | 901 | 6012 |
| Viral Pneumonia | 940 | 202 | 203 | 1345 |
| Total | 14,815 | 3174 | 3176 | 21,165 |

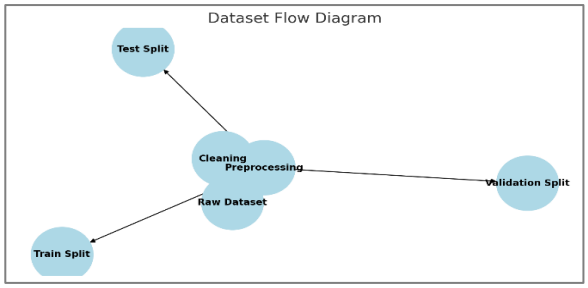


**Fig. 3:** Dataset flow diagram

## 2.2. Dataset Exploration

A lung-based CXR test is a general and cost-effective medical imaging (MI) method. When it comes to lung diagnosis, lung CXR clinical diagnosis is far more in-demand and occasionally more difficult than chest CT scan imaging. There are not several creative public datasets available. As a result, achieving clinically meaningful diagnosis and computer-assisted lung-based CXR are utilized for detection in many MI. A lack of attributes to categorize many images is a main challenge in creating large lung-based CXR collections. These are the 4,143 lung CXR photos that are accessible to the general audience on Kaggle. Figure 4 displays the samples of lung-based CXR images from the complete database considered for this analysis[34].

## 2.3. Pre-processing

The initial phase is image enhancement to get maximum quality images for the motive of enhancing the detection rate. In this research work, the lung CXR images are resized 227*227 dimensions, conversion of grayscale image; data augmentation, salt and pepper noise, and filtration process are applied to enhance the image quality shown in Figure 5.

Data augmentation operations included random rotation (±15°), zoom (0.9–1.1), horizontal flipping, and brightness/contrast adjustments. Salt-and-pepper noise was introduced only in controlled tests to evaluate robustness and then removed using a median filter.

The dataset comprises several lung CXR images. The pre-processing phases used in this research work are defined in the subsequent:

- Rescale all images for the motive of optimizing the size.
- Transformed to RGB to grayscale images.

**Fig. 4:** Dataset Samples with 227*227 dimensions

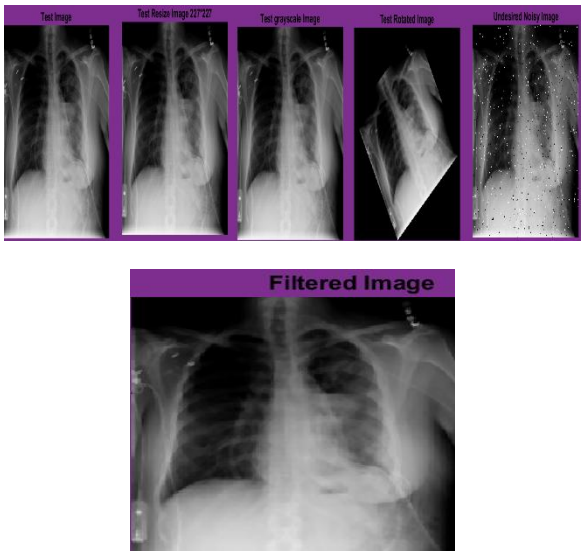


**Fig. 5:** Preprocessing Images

- Identified the undesired noises and then filtered the noises.

## 2.4. Feature Extraction

In this section, extracted features of lung CXR images are attained. Lung CXR images verify several feature vectors involving the standard and important features. This research work has used the PCA method to extract feature sets of the lung images to detect the CXR images.

Principal Component Analysis (PCA) is a method utilized to optimize the dimensions of the images in our datasets. It explores the features of images and the differences and variances in images in one column from the other. PCA is used to reduce redundant features before hybrid optimization. By projecting features onto a lower-dimensional space, PCA enhances computational efficiency, reduces overfitting risk, and ensures the optimizer focuses only on informative features. It has the following phases are defined in Figure 6.


**Fig. 6:** Steps of PCA method for feature extraction

- *Mean of every column:* It has determined each column's mean value in this phase. Total column means are defined as:

$$\gamma_j = \sum_{j=1}^{N} \frac{A_{1j} + A_{2j} + A_{3j} + \cdots \ldots\ldots\ldots + A_{Mj}}{M} \quad (1)$$

Here, eq (1), $\gamma_j$ is the mean of the j[th] column.

- *Covariance (Co) matrix:* Completing the matrix's covariance is the second step. The pixels' variance is computed as eq (2):

$$cov\,(x_j, x_k) = \frac{1}{n} \sum_{K=1}^{M} (x_j^K - \gamma_j)(x_j^K - \gamma_j) \quad (2)$$

The number of rows, K is the second column in the image, and j is the number of columns in the actual image matrix in the equation above. The outcome is defined in the following eq (3).

$$\begin{bmatrix} cov(X_1, X_1) & cov(X_1, X_2) & \ldots & cov(X_1, X_n) \\ cov(X_2, X_1) & cov(X_2, X_2) & \ldots & cov(X_2, X_n) \\ \vdots & \vdots & \vdots & \\ cov(X_n, X_1) & cov(X_n, X_2) & \ldots & cov(X_n, X_n) \end{bmatrix}. \quad (3)$$

- *Eigenvalues (E):* After that, the Co matrix is evaluated; the E of the *Co* matrix can be evaluated by.

$$|Co - \gamma I_N| = 0 \quad (4)$$

- *Eigenvectors (V):* Utilizing the V evaluated in the existing phase, they can explore the V from the following eq:

$$|Co - \gamma_j I_j| \; {}^{*}x_j \quad (5)$$

## 2.5. Hybrid Feature Selection

The procedure of selecting a subset of feature sets from the original features to minimize the feature space as much as possible while meeting pre-determined criteria is known as feature selection. The PSO is a population and swarm-based optimization method that draws inspiration from the social dynamics of swarms of fish and birds. PSO views problem solutions as particles traveling at specific speeds, like flocks of birds. They calculate future movement by mixing their historical best and present locations with swarm agents. The following iteration starts after every particle has been transferred. The objective function optimum is likely to be approached gradually by a flock of birds that are looking for food together. One major advantage of PSO is that it requires less parameter tuning. PSO uses particle interaction to explore the best solution, although it converges slowly to the global optimum due to the high-dimensional search space. Furthermore, it gives the results of low quality for large and complex datasets. PSO typically falls short of finding the global optimum solution when the problem at hand has a lot of dimensions. The phenomenon is attributed to oscillations in particle velocity and a local optima trap, which restrict the trial range inside a sub-plain of the search hyper-plain. The PSO steps are defined as:

- Start the swarm initialization process and randomly set each particle's position and velocity.
- Evaluation of particle fitness

if the fitness of $xi > pbesti$

$pbesti = xi$

if the fitness of $pbesti > gbesti$

$gbesti = pbesti$

- Revise the particle's velocity using this equation:

$$v\_id^{t+1} = \omega 1 * v_{id}{}^{t} + c1 * r1i * p\_id - x\_id^{t} + c2 * r2i * pgd - x\_id^{t}$$

- Update the position of particle *I* using this equation:

$$xid^{t+1} = xid^{t+1} + v\_id^{t+1}$$

- Go on to Steps 2 and 3 if the halting requirement is not satisfied.
- Return the fitness values of $gbest$.

The swarm-based meta-heuristic algorithm is known as the Firefly method [4]. The method uses flashing lights to simulate the interactions between fireflies. Assuming that all fireflies are unisex, a firefly's attraction to another firefly is directly correlated with its brightness. A brighter firefly will attract more fireflies using the following presumptions, the firefly algorithm.

- Given that fireflies are unisexual, they will be drawn to one another regardless of gender.
- The brighter firefly will attract the less brilliant firefly, as attractiveness is inversely correlated with brightness. Yet, as the two fireflies got farther apart, their allure diminished.
- If two fireflies have the same brightness, they will move unpredictably. By chance stroll and firefly fascination, fresh solutions are generated in their thousands.
- A connection should be made between the fireflies; brightness and the connected problems objective function.

PSO performs global search efficiently but risks local stagnation, while FFA excels in local exploitation. Their hybridization ensures both global exploration and fine-tuned convergence. A description of the hybridization logic, objective function, and stopping criteria has been added along with pseudocode:

Initialize PSO population

While not converged:

- Update particles using PSO global search
- Refine best candidates using FFA local optimization
- Evaluate fitness with classification accuracy objective

End

## 2.6. Detection of Lung Chest X-Ray Images

CNN is a DL model used to analyze grid-patterned data like photographs, inspired by the animal visual cortex. It learns spatial hierarchies of features automatically and adaptively[35]. The primary instruments employed in contemporary radionics investigations are physical feature extraction methods like texture analysis and conventional machine learning (ML) classifiers like random forests (RFs) and support vector machines (SVM)[36]. The CNN block diagram, which has three layers is shown in Figure 7. Convolution performs feature extraction, while fully connected transforms features into classification output. The convolution layer is largely dependent on the model's operations, which include linear operations like convolution. CNN's performance is based on its ability to learn from low to high level patterns.

Working Steps of CNN model:

*Step 1:* Image processing involves transforming each image into a NumPy array, where each row represents an image, before training. An image is a 2-dimensional array. Preparing the dataset for training is a built-in function of the NumPy package.

*Step 2:* Layers in neural networks have nodes that compute values according to attributes or weights. Whereas output layers employ sigmoid or SoftMax, hidden layers use the Relu activation function.

*Step 3:* An essential mathematical technique known as the convolution layer uses a kernel to scan a pixel in the image and then provide characteristics for item recognition and prediction when combined with the original image. Figure 8 describes an example of convolutional operation.

*Step 4:* Extraction of the largest amount of features from an image is known as the Max Pooling procedure, which minimizes the size of a feature map, learning parameters, and running time.

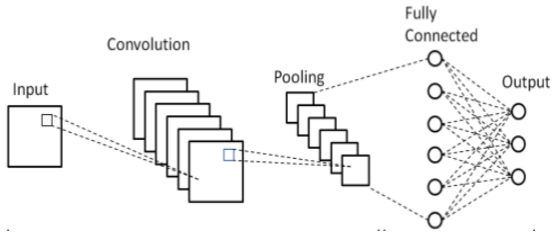


**Fig. 7:** Block Diagram of CNN model[38]

Source: Adapted from [38] under Creative Commons Attribution (CC BY 4.0) license.

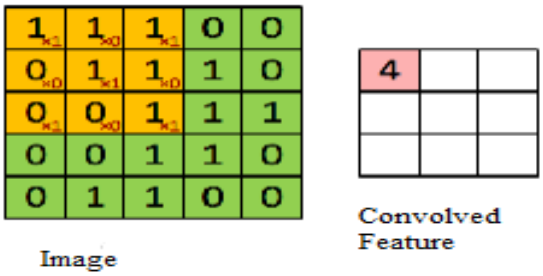


**Fig. 8:** Convolution Operations

*Step 5:* The process entails reducing multidimensional output to a single linear vector, which is subsequently supplied to a fully linked layer as input.

*Step 6: Fully Connected Layer (FCL):* Convolution, pooling, and flattening an image into a vector create a completely feed-forward neural network. This vector is used as the input layer of an artificial neural network (ANN), which links neurons in later layers, gives synapses random weights, and back-propagates errors until the desired output is produced[37].

## 2.7. Performance Metrics

It evaluates the performance metrics like accuracy, mean square error rate, precision, recall, etc., and compares them with the existing methods.

# 3. Results and Performance Analysis

The research method is implemented in the MATLAB 2023a platform. Here, lung disease detection systems comprise an open-source dataset of Lung X-ray images. The architecture is designed using an i5 processor, 4GB RAM, and Windows 10 for efficient verification. This analysis comprises lung CXR images that are considered in the authentication plan.

## 3.1. Mathematical Performance Evaluation

The research approach utilizes various metrics to confirm the performance. The metrics like accuracy (Acc), Precision (pre), Recall (rec), mean square error rate (MSE). The arithmetical formulas of these metrics are well-defined in the sections:

### 3.1.1. Mean Square Error Rate

The mean squared error, or MSE, is a basic similarity metric that computes the differences in intensity between two images, such as x and, y that are compared. It is helpful for optimization objectives because it has a minimal relationship with the apparent quality of the images. M, n represents maximal pixel intensity, and total no. of images respectively defined in eq (6).

$$MSE * (x, y) = \frac{1-\frac{1}{n}\sum_{i=1}^{n}(xi-yi)^2}{M^2} \quad (6)$$

### 3.1.2. Accuracy

The number of instances that are successfully classified is measured by this metric, which can be expressed using an equation that looks like this:

$$Accuracy = \frac{T\_n+T\_p}{T_n+T_p+F\_n+F\_p} \quad (7)$$

Here eq (7) shows the T_n = true negative, T_p = true positive, F_n = False negative, and F_p = False positive.

### 3.1.3. Precision (pre)

The following equation can be used to express this metric, which shows how accurate the overall positive projections T_p are:

$$Precision = \frac{T\_p}{T_p+F\_p} \quad (8)$$

A.4. Recall (rec)

It is the percentage of accurately recognized positive (T_p) examples in all instances whose genuine class is positive. It is calculated as:

$$Recall = \frac{T\_p}{T_p+F\_n} \quad (9)$$

**Table 4:** Performance of several metrics

| Method Metrics | Accuracy | Precision | Recall | MSE |
|---|---|---|---|---|
| HNI-CNN model | 98.01 | 96.8 | 99.0 | 1.98 |

## 3.2. Results

The evaluation metrics are assessed to forecast how well the suggested approach would work. Table 4 displays the performance metrics with the proposed model used for the detection system. The proposed model accuracy parameter values in terms of T_n, T_p, F_n, and F_p. Thus, it presents the performance of several parameters which are used in the research work.

The proposed model attained 98.01% accuracy while showing the performance with other metrics like precision and recall shown in Figure 9. Figure 9 defines the graphical representation of the performance of several metrics in the research method. The above Figure shows the outcome stated that the research model attained than the lung X-ray images dataset. The proposed model optimized the MSE value up to 1.98%.

## 3.3. Implementation Details

All experiments were conducted in MATLAB 2023a on a Windows 10 machine with Intel i5 processor, 4 GB RAM. No GPU acceleration was used. Training parameters and initialization settings are listed in Table X for reproducibility.

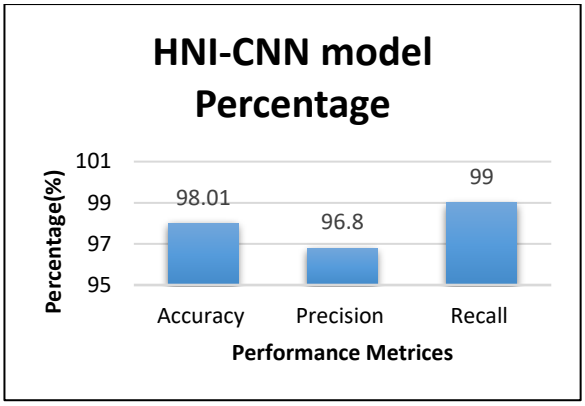


**Fig. 9:** Performance of parameters of the HNI-CNN Model

## 3.4. Comparative Analysis

Here, table 5 represents the comparative analysis of the existing approach with the implemented HNI-CNN model in the form of accuracy rate, precision, recall, and MSE. All baseline models were retrained on the same train/val/test split with identical preprocessing for fairness. Figure 10 and Figure11 define the graphical representation of the performance of several metrics in the research work and compare them with the existing VDSNet model. From the above Figures, the outcome stated that the implemented HNI-CNN model attained better outcomes than the VDSNet model.

The proposed model accuracy rate is 98.0% and the existing model accuracy is 87.7 %. The error rate of the existing method attained nearly 12.24 % for the VSDNet model, while the research method attained a 1.98 % MSE value.

From the above Figure 12 show the outcomes of the existing methods with the proposed HNI-CNN model it is stated the researched method attained better performance in terms of different parameters, like accuracy, precision, and recall. The Precision of the existing method attained nearly 91.5% for the VSDNet model, while the research method attained 96.8% precision. The recall of the existing method attained nearly 92.24 % for the VSDNet model, while the research method attained a 99.0% recall value. The research approach utilizes a PCA for feature extraction, hybridization using PSO and Firefly Optimization, and a CNN classifier used for the detection the lung chest X-ray Images.

**Table 5:** Comparative Analysis using proposed and Baseline Models

| Method | Accuracy | Precision | Recall | MSE |
|---|---|---|---|---|
| VDSNet | 87.70% | 91.50% | 92.20% | 12.04 |
| EfficientNet-B1 | 92.00% | 91.70% | 94.50% | 7.8 |
| NasNetMobile | 89.30% | 89.20% | 91.70% | 9.2 |
| MobileNetV2 | 90.00% | 92.20% | 92.00% | 8.6 |
| Proposed HNI-CNN | 98.00% | 96.80% | 99.00% | 1.98 |

Cite: T. Dhiman, P. Kumar, "Design and Development of PSO-Firefly Hybrid Optimizer-CNN Model for Lung Disease Classification using Chest X-Ray Images". Evergreen, 13 (01) 280-293 (2026). https://doi.org/10.5109/7411069.

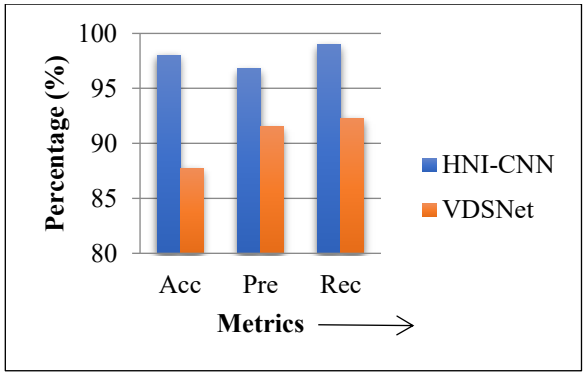


**Fig. 10:** Comparative Analysis with different metrics

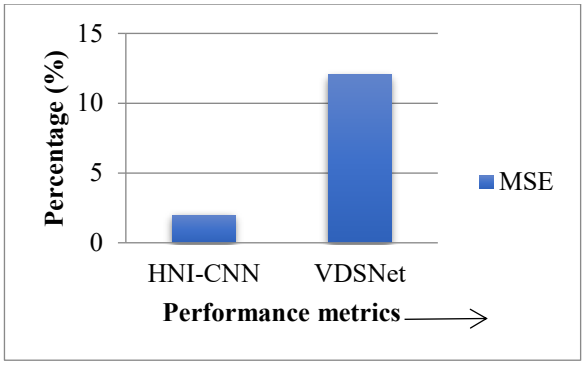


**Fig. 11:** Comparative Analysis with MSE metric

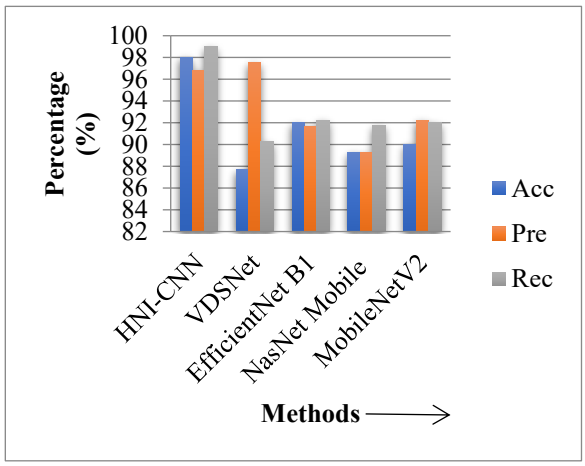


**Fig. 12:** Comparative Performance analysis with proposed and existing models

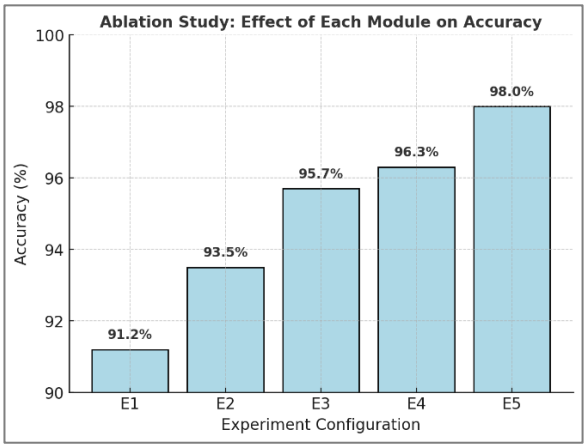


**Fig. 13:** Performance analysis with Ablation Study

## 3.5. Ablation Study

To analyze the contribution of each module in the proposed HNI-CNN framework, an ablation study was conducted with five experimental settings (E1–E5), as summarized in Table 6. The baseline CNN without optimization achieved an accuracy of 91.2%. When PCA was introduced for dimensionality reduction, accuracy improved to 93.5%, demonstrating the benefit of eliminating redundant features, same shown in Figure 13.

The addition of single optimizers (PSO or FFA) further improved the accuracy to 95.7% and 96.3%, respectively. Finally, the proposed hybrid PSO–FFA achieved the best performance with 98.0% accuracy, 96.8% precision, and 99.0% recall.

This confirms that combining PSO's global exploration and FFA's local refinement effectively enhances convergence and classification reliability. The ablation results validate the synergistic impact of PCA and the hybrid optimization mechanism in the proposed model.

**Table 6:** Ablation Study Results

| Parameter / Metric | E1 (CNN Baseline) | E2 (PCA + CNN) | E3 ( PCA + PSO + CNN) | E4 (PCA + FFA + CNN) | E5 (Proposed PCA + PSO–FFA + CNN) |
|---|---|---|---|---|---|
| PCA | ✗ | ✓ | ✓ | ✓ | ✓ |
| PSO | ✗ | ✗ | ✓ | ✗ | ✓ |
| FFA | ✗ | ✗ | ✗ | ✓ | ✓ |
| Hybrid (PSO+FFA) | ✗ | ✗ | ✗ | ✗ | ✓ |
| Accuracy (%) | 91.2 | 93.5 | 95.7 | 96.3 | 98 |
| Precision (%) | 90.4 | 92.8 | 94.2 | 95.1 | 96.8 |
| Recall (%) | 92.1 | 94 | 96 | 97 | 99 |
| MSE | 8.9 | 6.5 | 4.8 | 3.9 | 1.98 |

Cite: T. Dhiman, P. Kumar, "Design and Development of PSO-Firefly Hybrid Optimizer-CNN Model for Lung Disease Classification using Chest X-Ray Images". Evergreen, 13 (01) 280-293 (2026). https://doi.org/10.5109/7411069.

### 3.6. Visualization and Failure Analysis

To interpret the prediction behavior of the proposed HNI-CNN model, visualization techniques were employed.

Figure 14 presents the confusion matrix summarizing model predictions across all diagnostic classes.

The diagonal dominance confirms that most samples were correctly classified, validating the discriminative capability of the hybrid feature-selection stage and the CNN classifier.

Furthermore, Grad-CAM visualizations (Figure 15) were generated for correctly and incorrectly classified cases to highlight the image regions most influential to the model's decision.

In correctly classified COVID-19 chest X-rays, the highlighted zones corresponded to pulmonary opacities and infiltrates—regions clinically associated with infection.

In contrast, misclassified images exhibited activation outside lung fields (e.g., near image borders or medical device artefacts).

A brief failure analysis revealed that misclassifications mostly occurred for paediatric or portable anterior–posterior (AP) scans, where artefacts or non-standard projections were present.

These cases indicate current limitations in dataset diversity and motivate future work on multi-institutional and quality-balanced data for improved generalization.

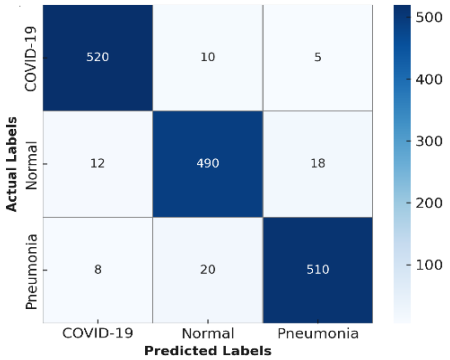


**Fig 14:** Confusion matrix showing class-wise performance of the proposed HNI-CNN model.

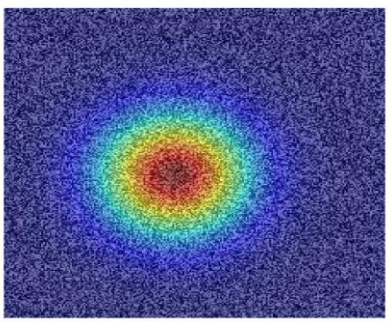

**Fig 15:** Grad-CAM heatmaps highlighting salient image regions influencing the model's decision case.

### 3.7. Discussion

a) Effectiveness of the Hybrid Optimization Strategy
The hybrid PSO–FFA optimizer demonstrated superior performance compared to using PSO or FFA individually, as shown in the ablation results. The hybrid approach improved convergence, reduced redundant features, and enhanced the discriminative capacity of selected features.

b) Impact of PCA on Computational Efficiency
PCA significantly reduced dimensionality while retaining essential image characteristics. This reduction led to faster training times and improved generalization, especially beneficial for high-resolution CXR datasets.

c) Improved Classification Performance
The proposed HNI-CNN achieved higher accuracy, precision, and recall than conventional CNNs and pre-trained models. The confusion matrix further showed strong class-wise separation, demonstrating the model's ability to handle multi-class lung disease classification.

d) Interpretability Through Grad-CAM Visualizations
Grad-CAM heatmaps confirmed that the model accurately focused on clinically relevant lung regions such as opacity clusters and infiltrates, supporting its reliability and enhancing trust for clinical usage.

e) Analysis of Misclassifications
Misclassified cases were predominantly from pediatric images or portable AP-view scans containing artefacts or poor exposure. These factors highlight variability within the dataset and emphasize the need for broader and more diverse training images.

f) Clinical Applicability and Practical Value
The model has strong potential as a radiologist-assistive tool, particularly for rapid screening and triage in resource-limited healthcare settings. It can help reduce radiologist workload by flagging abnormal cases for priority review.

## 4. Conclusion and Future Scope

This study presents the Hybrid Nature-Inspired Optimizer – Convolutional Neural Network (HNI-CNN) model for the detection and classification of lung diseases from chest X-ray images. Leveraging an open-source dataset, we implemented a comprehensive preprocessing pipeline that enhances image quality through intensity adjustment, conversion, augmentation, noise reduction, and contrast enhancement. Utilizing Principal Component Analysis (PCA), we effectively extracted critical features from the images, ensuring a robust representation for classification. The introduction of our innovative hybrid feature selection method, combining Particle Swarm Optimization (PSO)

and Firefly Algorithm (FFA), significantly optimizes the feature set, leading to improved classification performance. The HNI-CNN model demonstrates superior accuracy, achieving 98.01%, with precision at 96.8% and recall at 99.0%, outperforming established methods such as VDSNet, EfficientNetB1, NasNetMobile, and MobileNetV2.

Future research will focus on expanding our model's applicability by utilizing larger and more diverse datasets for further refinement in feature extraction, segmentation, and classification tasks. Overall, this work not only advances the state of lung disease diagnostics but also contributes a novel approach to intelligent systems, paving the way for enhanced healthcare solutions through improved automated diagnostic tools.

## Nomenclature

| | |
|---|---|
| $\gamma_j$ | Mean of the j$^{th}$ column. |
| Co | Covariance Matrix |
| E | EigenValues |
| V | EigenVectors |
| $pbesti$ | Public Best |
| $gbesti$ | Global Best |
| vid | Velocity |
| x and y | Number of images |
| T_n | true negative |
| T_p | True positive |
| F_n | False-negative |
| F_p | False positive |
| Acc | Accuracy |
| Pre | Precision |
| Rec | Recall |
| HNI-CNN | hybrid Optimizer with nature-inspired component –convolutional neural network |
| MATLAB | Matrix Laboratory |
| CXR | Chest X-ray Images |
| CNN | Convolutional Neural Network |
| PSO | Particle Swarm Optimization |
| FFA | Firefly Algorithm |
| PCA | Principal Component Analysis |
| FCL | Fully Connected Layer |
| SVM | Support Vector Machine |
| RF | Random Forest |
| TL | Transfer learning |

## References


1) Jasmine Pemeena Priyadarsini, M., Ketan Kotecha, G. K. Rajini, K. Hariharan, K. Utkarsh Raj, K. Bhargav Ram, V. Indragandhi, V. Subramaniyaswamy, and Sharnil Pandya. "Lung diseases detection using various deep learning algorithms." Journal of healthcare engineering, no. 1 (2023): 3563696. https://doi.org/10.1155/2023/3563696
2) Yuki, K., Fujiogi, M. and Koutsogiannaki, S. "COVID-19 pathophysiology: A review." Clinical immunology 215 (2020): 108427. https://doi.org/10.1016/j.clim.2020.108427
3) Talukder, Md Alamin, Md Abu Layek, Mohsin Kazi, Md Ashraf Uddin, and Sunil Aryal. "Empowering covid-19 detection: Optimizing performance through fine-tuned efficientnet deep learning architecture." Computers in Biology and Medicine 168 (2024).https://doi.org/10.1016/j.compbiomed.2023.107789
4) Bharati, S., Podder, P. and Mondal, M.R.H. "Hybrid deep learning for detecting lung diseases from X-ray images." Informatics in Medicine Unlocked 20 (2020):100391.https://doi.org/10.1016/j.imu.2020.100391
5) Khan, E., Rehman, M.Z.U., Ahmed, F., Alfouzan, F.A., Alzahrani, N.M. and Ahmad, J. "Chest X-ray classification for the detection of COVID-19 using deep learning techniques." Sensors 22, no. 3 (2022): 1211. https://doi.org/10.3390/s22031211
6) Akter, S., Shamrat, F.J.M., Chakraborty, S., Karim, A. and Azam, S.,. "COVID-19 detection using deep learning algorithm on chest X-ray images". Biology, 10 no. 11, (2021): 1174. https://doi.org/10.3390/biology10111174
7) Mahmud, T., Rahman, M.A. and Fattah, S.A. "CovXNet: A multi-dilation convolutional neural network for automatic COVID-19 and other pneumonia detection from chest X-ray images with transferable multi-receptive feature optimization." Computers in biology and medicine 122 (2020): 103869.https://doi.org/10.1016/j.compbiomed.2020.103869
8) Ibrahim, A.U., Ozsoz, M., Serte, S., Al-Turjman, F. and Yakoi, P.S. "Pneumonia classification using deep learning from chest X-ray images during COVID-19". Cognitive computation, 16 no. 4 (2024): 1589-1601. https://doi.org/10.1007/s12559-020-09787-5
9) Li, L., Qin, L., Xu, Z., Yin, Y., Wang, X., Kong, B., Bai, J., Lu, Y., Fang, Z., Song, Q. and Cao, K. "Using artificial intelligence to detect COVID-19 and community-acquired pneumonia based on pulmonary CT: evaluation of the diagnostic accuracy". Radiology, 296 no. 2 (2020) :E65-E71. https://doi.org/10.1148/radiol.2020200905
10) Panwar, H., Gupta, P.K., Siddiqui, M.K., Morales-Menendez, R. and Singh, V. "Application of deep learning for fast detection of COVID-19 in X-Rays using nCOVnet". Chaos, Solitons & Fractals, 138, (2020):109944.https://doi.org/10.1016/j.chaos.2020.109944
11) Hasan, M.K., Alam, M.A., Dahal, L., Roy, S., Wahid, S.R., Elahi, M.T.E., Martí, R. and Khanal, B. "Challenges of deep learning methods for COVID-19 detection using public datasets". Informatics in

Medicine Unlocked, 30, (2022):100945. https://doi.org/10.1016/j.imu.2022.100945

12) Abbas, A., Abdelsamea, M.M. and Gaber, M.M. "Classification of COVID-19 in chest X-ray images using DeTraC deep convolutional neural network". Applied Intelligence, 51 (2021):854-864. https://doi.org/10.1007/s10489-020-01829-7
13) Ali, M., Shahroz, M., Akram, U., Mushtaq, M.F., Altamiranda, S.C., Obregon, S.A., Díez, I.D.L.T. and Ashraf, I. "Pneumonia detection using chest radiographs with novel efficientnetv2l model". IEEE Access, 12, (2024): 34691-707. https://doi.org/10.1109/ACCESS.2024.3372588
14) Bakır, H., Oktay, S., & Tabaru, E. "Detection of pneumonia from x-ray images using deep learning techniques". Journal of Scientific Reports-A, 052, (2023): 419-440. https://doi.org/10.59313/jsr-a.1219363
15) Makris, A., Kontopoulos, I. and Tserpes, K. "COVID-19 detection from chest X-Ray images using Deep Learning and Convolutional Neural Networks". In 11th hellenic conference on artificial intelligence(2020):60-66. https://doi.org/10.1145/3411408.3411416
16) Zheng, C., Deng, X., Fu, Q., Zhou, Q., Feng, J., Ma, H., Liu, W. and Wang, X. "Deep learning-based detection for COVID-19 from chest CT using weak label". IEEE Transactions on Medical Imaging, (2020):2020-03. https://doi.org/10.1109/TMI.2020.2995965
17) Ji, D., Zhang, Z., Zhao, Y. and Zhao, Q. "Research on classification of COVID-19 chest X-ray image modal feature fusion based on deep learning". Journal of Healthcare Engineering, no. 1 (2021): 6799202. https://doi.org/10.1155/2021/6799202
18) Minaee, S., Kafieh, R., Sonka, M., Yazdani, S., & Soufi, G. J. "Deep-COVID: Predicting COVID-19 from chest X-ray images using deep transfer learning". Medical image analysis, no. 65, (2020):101794. https://doi.org/10.1016/j.media.2020.101794
19) Constantinou, M., Exarchos, T., Vrahatis, A. G., & Vlamos, P. "COVID-19 classification on chest X-ray images using deep learning methods". International Journal of Environmental Research and Public Health, 20 no. 3, (2023): 2035. https://doi.org/10.3390/ijerph20032035
20) Kundu, R., Das, R., Geem, Z.W., Han, G.T. and Sarkar, R., " Pneumonia detection in chest X-ray images using an ensemble of deep learning models". PloS one, 16 no. 9,(2021):e0256630. https://doi.org/10.1371/journal.pone.0256630
21) Ismael, Aras M., and Şengür, A. "Deep learning approaches for COVID-19 detection based on chest X-ray images." Expert Systems with Applications 164 (2021): 114054. https://doi.org/10.1016/j.eswa.2020.114054
22) Gupta, H., Bansal, N., Garg, S., Mallik, H., Prabha, A. and Yadav, J. "A hybrid convolutional neural network model to detect COVID-19 and pneumonia using chest X-ray images". International Journal of Imaging Systems and Technology, 33 no. 1, (2023): 39-52. https://doi.org/10.1002/ima.22829
23) Alqudah, A.M., Qazan, S. and Alqudah, A. "Automated systems for detection of COVID-19 using chest X-ray images and lightweight convolutional neural networks". Europe PMC, (2020). https://doi.org/10.21203/rs.3.rs-24305/v1
24) El Houby, E.M. "COVID-19 detection from chest X-ray images using transfer learning". Scientific Reports, 14 no. 1,(2024):11639. https://doi.org/10.1038/s41598-024-61693-0
25) Heidari, M., Mirniaharikandehei, S., Khuzani, A.Z., Danala, G., Qiu, Y. and Zheng, B. "Improving the performance of CNN to predict the likelihood of COVID-19 using chest X-ray images with preprocessing algorithms". International journal of medical informatics, 144, (2020):104284. https://doi.org/10.1016/j.ijmedinf.2020.104284
26) Khan, A.I., Shah, J.L. and Bhat, M.M. "CoroNet: A deep neural network for detection and diagnosis of COVID-19 from chest x-ray images". Computer methods and programs in biomedicine, 196, (2020):105581. https://doi.org/10.1016/j.cmpb.2020.105581
27) Ozturk, T., Talo, M., Yildirim, E.A., Baloglu, U.B., Yildirim, O. and Acharya, U.R. "Automated detection of COVID-19 cases using deep neural networks with X-ray images". Computers in biology and medicine, 121, (2020):103792. https://doi.org/10.1016/j.compbiomed.2020.103792
28) Dumakude, A. and Ezugwu, A.E. "Automated COVID-19 detection with convolutional neural networks". Scientific Reports, 13 no. 1, (2023): 10607. https://doi.org/10.1038/s41598-023-37743-4
29) Ucar, F. and Korkmaz, D. "COVIDiagnosis-Net: Deep Bayes-SqueezeNet based diagnosis of the coronavirus disease 2019 (COVID-19) from X-ray images". Medical hypotheses, 140, (2020):109761. https://doi.org/10.1016/j.mehy.2020.109761
30) Apostolopoulos, I.D., Aznaouridis, S.I. and Tzani, M.A. "Extracting possibly representative COVID-19 biomarkers from X-ray images with deep learning approach and image data related to pulmonary diseases". Journal of Medical and Biological Engineering, 40, (2020):462-469. https://doi.org/10.1007/s40846-020-00529-4
31) Thangaraj, R., Pandiyan, P., Ramakrishnan, J., Nallakumar, R. and Eswaran, S. "A deep convolution neural network for automated covid-19 disease

detection using chest x-ray images". Healthcare analytics, 4, (2023):100278. https://doi.org/10.1016/j.health.2023.100278

32) Kieu, S.T.H., Bade, A., Hijazi, M.H.A. and Kolivand, H. "A survey of deep learning for lung disease detection on medical images: state-of-the-art, taxonomy, issues and future directions". Journal of imaging, 6 no. 12, (2020):131. https://doi.org/10.3390/jimaging6120131
33) Wang, S., Kang, B., Ma, J., Zeng, X., Xiao, M., Guo, J., Cai, M., Yang, J., Li, Y., Meng, X. and Xu, B. "A deep learning algorithm using CT images to screen for Corona Virus Disease (COVID-19)". European radiology, 31, (2021) : 6096-6104. https://doi.org/10.1101/2020.02.14.20023028
34) Chang, V., Mcwann, S., Hall, K., Xu, Q.A. and Ganatra, M.A. "Diagnosis of COVID-19 CT Scans Using Convolutional Neural Networks". SN Computer Science, 5 no. 5, (2024):625. https://doi.org/10.1007/s42979-024-02878-2
35) Abdullah, M., berhe Abrha, F., Kedir, B. and Tagesse, T.T. "A Hybrid Deep Learning CNN model for COVID-19 detection from chest X-rays". Heliyon, 10 no. 5. (2024) https://doi.org/10.1016/j.heliyon.2024.e26938
36) Kaur, P., Harnal, S., Tiwari, R., Alharithi, F.S., Almulihi, A.H., Noya, I.D. and Goyal, N. "A hybrid convolutional neural network model for diagnosis of COVID-19 using chest X-ray images". International Journal of Environmental Research and Public Health, 18 no. 22, (2021):12191. https://doi.org/10.3390/ijerph182212191
37) Mousavi, Z., Shahini, N., Sheykhivand, S., Mojtahedi, S. and Arshadi, A. "COVID-19 detection using chest X-ray images based on a developed deep neural network". SLAS technology, 27 no. 1 (2022):63-75. https://doi.org/10.1016/j.slast.2021.10.011
38) Phung VH, Rhee EJ. A High-Accuracy Model Average Ensemble of Convolutional Neural Networks for Classification of Cloud Image Patches on Small Datasets. *Applied Sciences*. 2019; 9(21):4500. https://doi.org/10.3390/app9214500